

## Low intensity solar flares' impact: numerical modeling

A. Kolarski<sup></sup>, V.A. Srećković<sup></sup> and F. Arnaut<sup></sup>

*Institute of Physics Belgrade, University of Belgrade, Pregrevica 118,  
11080 Belgrade, Serbia (E-mail: [aleksandra.kolarski@ipb.ac.rs](mailto:aleksandra.kolarski@ipb.ac.rs))*

Received: September 29, 2023; Accepted: October 26, 2023

**Abstract.** Solar flares, as strong explosions on the Sun's surface, are well known driving agents that severely affect the near-Earth environment, producing additional ionization within the sunlit Earth's atmospheric layers. X-ray solar flares can be classified regarding their effects on the lower ionosphere and its electron density profile. The focus of this research is on the study of disturbances induced by X-ray solar flares in order to predict the impact of possible weak solar events. In this paper we examined solar activity of lower intensity by conducting numerical modeling using several models and based on data obtained by very low frequency radio signals and from the Geostationary Operational Environmental Satellite (GOES) database on solar X-ray radiation.

**Key words:** Solar activity – Solar X-ray flares – Radio signal perturbations – GOES

### 1. Introduction

Solar flares (SFs) are powerful bursts of electromagnetic radiation originating from the Sun's surface [Bothmer et al. \(2007\)](#). Among the categories of SF from A to X-class, B- and C-class SFs represent a low to low-to-moderate level of intensity ([Grubor et al., 2008](#); [Hayes et al., 2021](#)). Although B- and C-class flares are considered to have low level intensity, they still possess the potential to cause disruptions in communication and navigation systems, if they are directed towards the Earth and especially during periods of quiet solar activity such as periods of solar minimum(s). During periods of solar minimum, which refers to the phase of the 11-year solar cycle with minimal solar activity, B- and C-class SFs become significant, as they often constitute the majority of solar flares observed in these periods.

Low class SFs, especially during periods of solar minimum, can induce disturbances in the ionosphere, leading to noticeable effects on terrestrial communication. The primary effect of SFs, in general, on the ionosphere is the augmentation in electron density. The intense X-ray and ultraviolet radiation released during SFs can ionize the upper atmosphere, creating additional free

electrons (Šulić et al., 2016; Curto, 2020; Žigman et al., 2007). These free electrons can affect radio wave propagation by altering the refractive properties of the ionosphere. As a result, the density of the ionosphere increases temporarily, influencing the behavior of radio signals passing through it (Kelly, 2009).

Very Low Frequency (VLF) technology plays a crucial role in studying solar flares and their effects on the lower ionosphere. VLF technology utilizes a range of electromagnetic waves with frequencies from 3 to 30 kHz, with the ability to propagate over long distances without losses and penetrate through both soil and water, making them bounce within the Earth-ionosphere waveguide (Ratcliffe et al., 1972; Silber & Price, 2017). VLF technology finds particular relevance in the study of solar flares due to its ability to capture and analyze the effects of SFs and to indirectly provide data of relevance to ionospheric plasma property variations during these events (Kolarski et al., 2011; Šulić & Srećković, 2014; Srećković et al., 2017; Arnaut et al., 2023). By observing such alterations, valuable insights into the Sun-Earth “connection” can be gained and an enhanced overall understanding of space weather phenomena. The study of SFs of low intensity during solar minimum and their impact on the ionosphere provides valuable insights into the complex interactions between Sun and Earth’s upper atmosphere (Barta et al., 2022; Grodji et al., 2022).

## 2. Observations

Transit between solar cycle (SC) 23 and 24 implies the period of solar activity is characterized by quiet Sun, i.e., solar minimum. The solar minimum of the 23/24 solar cycle often refers to the period mainly related to years 2008 and 2009, i.e. a period with quiet Sun between the descending branch of the SC 23 and the ascending branch of the SC 24. During this period there were not many SFs reported. More precisely only 8 C class SF events occurred in January, April, November and December and 1 M class SF occurred in March during 2008. Likewise 28 C class SF events occurred in July, September, October and December of 2009. When mutually compared in terms of background solar radiation, year 2008 was a bit calmer with X-ray background flux up to A8.1 compared to 2009 with X-ray background flux up to B1.4, but both of low background solar radiation conditions enabled studying of low class SFs and their influence on Earth’s ionosphere. Results of monitoring solar activity during the 23/24 solar minimum using VLF technology and the European mid-latitude lower ionospheric response to some of the low class SFs from this period based on records obtained by BEL VLF station in Belgrade (Serbia) and estimated electron densities using the Long Wave Propagation Capability (LWPC) methodology can be found in Kolarski et al. (2022a).

In this paper focus is on the utilization of two numerical methods, so called FlareED and easyFit that were developed by Srećković et al. (2021a,b) on the cases of low intensity SFs (lower C- and upper B-class SFs). Moreover the aim

of present paper is to test methods' efficiency and sensitivity when applied to cases of SFs from the lower part of the soft X-ray irradiance spectrum. We note that initially FlareED and easyFit methods were developed for SF events of mid to high intensity (upper C-, M- and lower X-class SFs, e.g. [Srećković et al. \(2021b\)](#); [Kolarski et al. \(2022b\)](#)).

**Table 1.** Estimated electron densities at nominal height of 74 km by employed different approaches: classical using LWPC, FlarED, easyFit and ML methods.

dd/mm/yyyy	27/10/2009	16/12/2009	23/12/2009
SF class	B8.3	C3.7	C6.4
max X-ray flux time (UT)	13:11	13:02	10:17
Ne LWPC ( $\text{m}^{-3}$ )	$3.79 \cdot 10^8$	$1.37 \cdot 10^9$	$1.17 \cdot 10^9$
Ne easyFit ( $\text{m}^{-3}$ )	$4.20 \cdot 10^8$	$1.01 \cdot 10^9$	$2.33 \cdot 10^9$
Ne FlarED ( $\text{m}^{-3}$ )	$3.47 \cdot 10^8$	$9.64 \cdot 10^8$	$1.64 \cdot 10^9$
Ne ML ( $\text{m}^{-3}$ )	$4.20 \cdot 10^8$	$1.02 \cdot 10^9$	$2.28 \cdot 10^9$

Along with these two methods that were already used for purposes of exploring the influences of stronger SFs on mid-latitude lower ionospheric plasma properties and are used in this study as well, here we also present results from a novel numerical method relying on machine learning (ML) techniques that is applied to low intensity SFs. Machine learning (ML) techniques have demonstrated extensive applicability in various domains, including research, engineering, and industry. Therefore, these techniques offer significant informational value that is not readily identifiable through other statistical methods, thereby offering a novel perspective on the data. One prominent category of widely used algorithms comprises tree, or forest-based techniques, such as Random Forest (RF) ([Breiman, 2001](#)) or XGBoost (XGB) ([Chen & Guestrin, 2016](#)). A typical ML workflow involves the initial preparation of the training and testing datasets, which include both the features and the target variables. Subsequently, the model is trained using the train dataset, following which the evaluation phase can be initiated using the test dataset, i.e., testing the trained model on a test dataset and constructing evaluation metric statistics. Once satisfactory model (hyper)parameters have been obtained, the model can be utilized for predicting the target variable on other datasets. The XGB algorithm was utilized in this study to derive the  $\beta$  and  $H'$  parameters (the so called Wait's parameters, [Wait & Spies 1964](#)) (target variables; multi-output ML task) from X-ray irradiance data and other features that were derived from the statistical properties of the X-ray irradiance data (feature data). The XGB model was fine-tuned in relation to the number of trees and the learning rate.

From period 2008 - 2009 several days with reported X-ray solar activity were singled out and inspected in detail: 03 November 2008, 05 July 2009, 27 October 2009, 10 December 2009, 16 December 2009, 21 December 2009 and

23 December 2009. Days were primarily chosen for analysis based on reported X-ray SFs that were “visible” on BEL VLF recordings, in order to provide it possible to compare results related to estimated electron densities obtained by the classical approach (such as Kolarski et al. 2022a) and by using FlareED and easyFit methods for interpretable cases, on the one hand and to avoid cases of stronger C-class events on the other (like M1.7 on 25 March 2008 with max. X-ray flux at 18:56UT or C7.6 & C7.2 on 18 & 22 December 2009, with max. X-ray flux at 18:55UT & 04:56UT respectively).

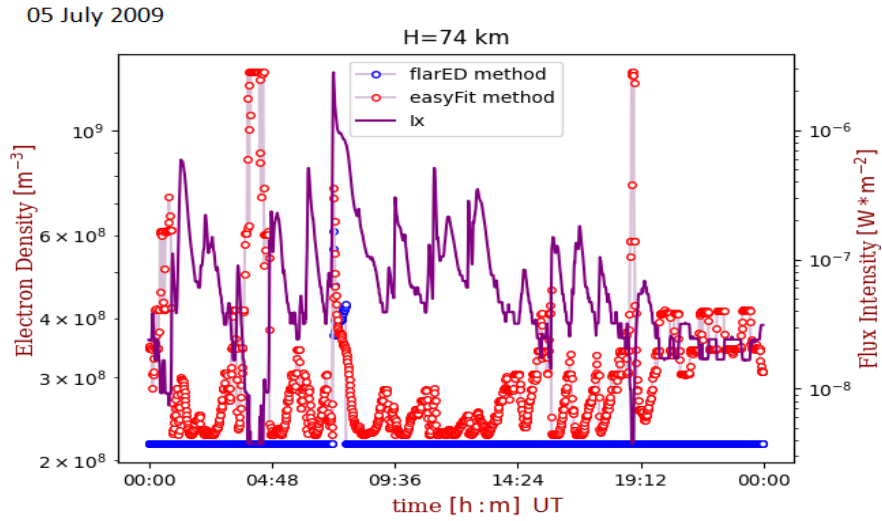


**Figure 1.** X-ray flux from GOES-15, and  $N_e$  ( $h = 74$  km) as a function of UT during 05 July 2009. The dashed line with circles shows results acquired by FlarED and easyFit methods.

During 03 November 2008, there were only 3 SFs reported with 2 of them of B-class with intensities in the range B2.4-2.9 and 1 of C-class of intensity C1.6, background flux was of A0.0 and sunspot number was 18. During 05 July 2009, there were 14 SFs reported with 13 of them of B-class with intensities in the range B1-5.9 and 1 of C-class of intensity C2.7, background flux was of A2.2 and sunspot number was 26. During 27 October 2009, there were 23 SFs reported with 18 of them of B-class with intensities in the range B1-8.4 and 5 of C-class with intensities in the range C1.1-1.7, background flux was of A4.2 and sunspot number was 29. During 10 December 2009, there were only 3 SFs reported with 2 of them of B-class with intensities in the range B1.4-6 and 1 of C-class of intensity C3.4, background flux was of A0.0 and sunspot number was 13. During 16 December 2009, there were 9 SFs reported with 6 of them of B-class with intensities in the range B3-8.6 and 3 of C-class with intensities in

the range C1.4-5.3, background flux was of B1.2 and sunspot number was 30. During 21 December 2009, there were 12 SFs reported with 10 of them of B-class with intensities in the range B1.6-8.6 and 2 of C-class with intensities in the range C1-2.5, background flux was of A9.3 and sunspot number was 42. During 23 December 2009, there were 5 SFs reported with 4 of them of B-class with intensities in the range B1.6-8.6 and 1 of C-class of intensity C6.4, background flux was of A7.5 and sunspot number was 23.

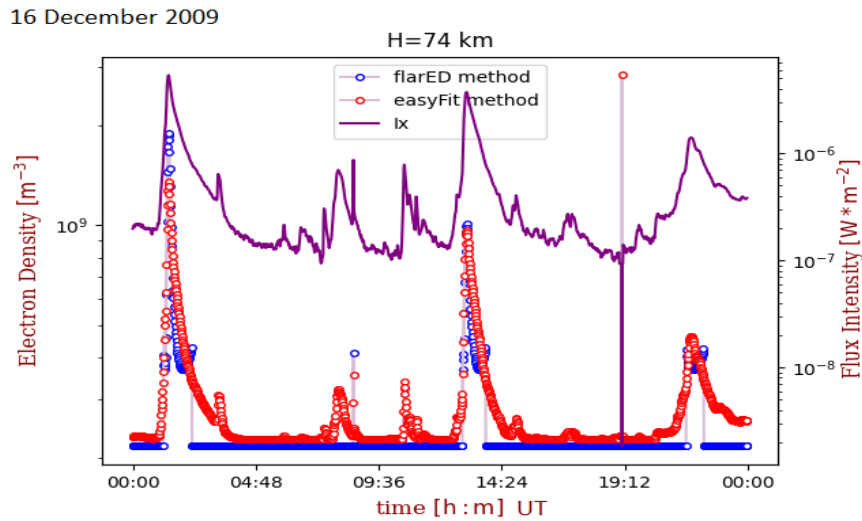


**Figure 2.** X-ray flux from GOES-15, and  $N_e$  ( $h = 74$  km) as a function of UT during 16 December 2009. The dashed line with circles shows results acquired by FlarED and easyFit methods.

### 3. Results and discussion

As previously mentioned, the factor of flare induced perturbation “visibility” on BEL VLF recordings was of prime significance. However, numerical methods FlareED and easyFit were conducted for chosen days in 24h continuity manner, in order to explore these events that were not “visible” in Belgrade due to nocturnal conditions. Figures 1-5 give an overview of the obtained results by application of numerical methods FlareED (blue) and easyFit (red) to the cases chosen for analysis. Aside from all previously mentioned factors, difference between the X-ray flux (violet) characteristic in terms of standalone SF events separated by periods with no activity and numerous back-to-back SFs was subject of interest in the conducted analysis as well. Solar soft X-ray flux is taken from Geostationary Operational Environmental Satellite (GOES) archive database (<https://satdat.ngdc.noaa.gov/sem/goes/data/avg/>).

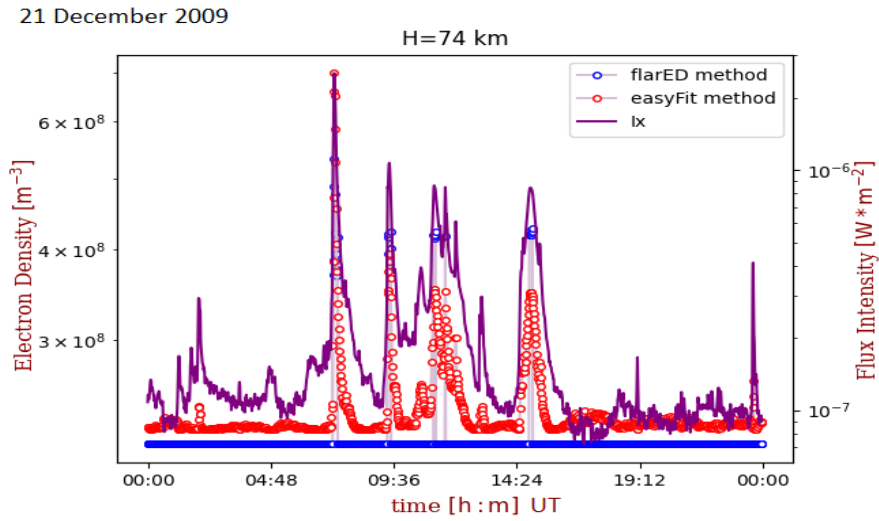


**Figure 3.** X-ray flux from GOES-15, and  $Ne$  ( $h = 74$  km) as a function of UT during 21 December 2009. The dashed line with circles shows results acquired by FlarED and easyFit methods.

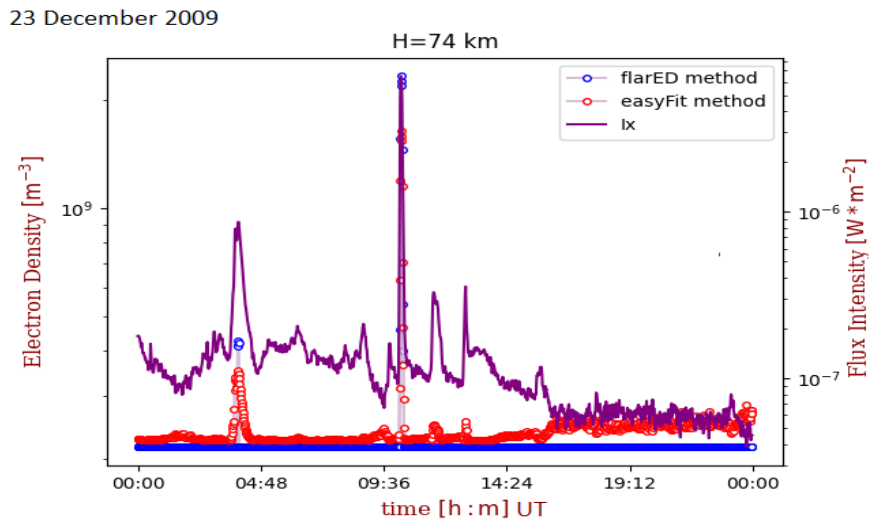


**Figure 4.** X-ray flux from GOES-15, and  $Ne$  ( $h = 74$  km) as a function of UT during 23 December 2009. The dashed line with circles shows results acquired by FlarED and easyFit methods.

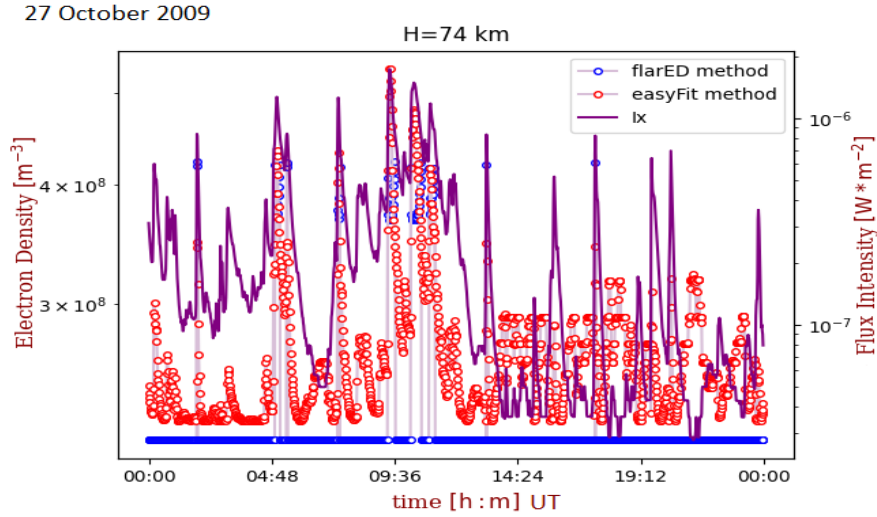


**Figure 5.** X-ray flux from GOES-15, and  $Ne$  ( $h = 74$  km) as a function of UT during 27 October 2009. The dashed line with circles shows results acquired by FlareED and easyFit methods.

In general, the easyFit method provided significantly more detailed insight in processed data in terms of sensitivity when applied on cases of low intensity X-ray SFs, in range of low B-class SFs to moderate C-class SFs of B1-C6.4, in terms of mimicking solar soft X-ray flux variation as compared to the FlareED method. FlareED method proven not to be sensitive to very low intensity SFs, giving practically unperturbed parameters as output in such cases. However, in cases of higher intensity SFs, FlareED method gave better results in terms of reaching maximal values in relation to peaks of solar soft X-ray flux variation. On the other hand, both methods gave either some false and/or positive-exaggerated output results. Both methods have proven to be more efficient in cases of more standalone SFs than these of high back-to-back occurrence, with the easyFit method superior in efficiency of recognizing X-ray flux outages, compared to FlareED method that showed no ability at all.

Results regarding electron densities at a nominal height of 74 km, as obtained by the application of classical approach based on NAA/24.0 kHz signal recordings from the Belgrade VLF database in the case of three X-ray SF events of low intensity: a) low intensity C-class solar flare event C3.7 from the 16 December 2009 at 13:02UT, b) moderate intensity C-class solar flare event C6.5 from the 23 December 2009 at 10:17UT and c) moderate intensity B-class solar flare event B8.35 from the 27 October 2009 at 13:11UT (Kolarski *et al.*, 2022a) are compared with the results obtained by application of numerical methods the

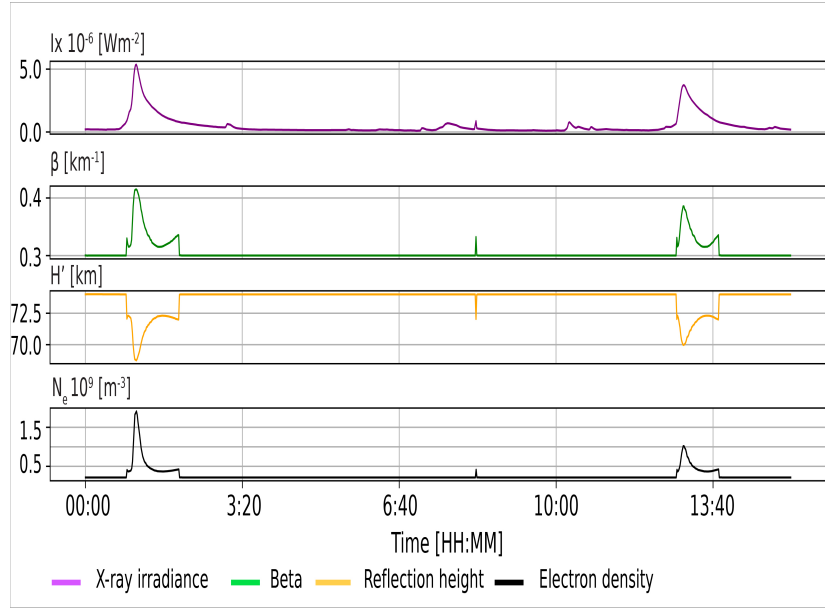


**Figure 6.** X-ray flux from GOES-15,  $\beta$  and  $H'$  parameters and  $N_e$  ( $h = 74$  km) as a function of UT during 16 December 2009 as results acquired by method relying on ML.

FlareED and the easyFit in the case of these SF events and presented in Table 1. In the case of the B8.3 SF, the lowest in intensity of these three SFs, both methods gave electron density of the same order of magnitude, with the result from the easyFit method slightly overestimated and from the FlarEd method slightly underestimated compared to one from the classical approach, with the result from the FlarEd method closer in absolute value. In the case of C3.7 SF, medium in strength of these three SFs, both methods gave electron density underestimated compared to one from classical approach, with the result obtained from the easyFit method closer in absolute value. In the case of C6.4, the highest in strength of these three SFs, both methods gave electron density of the same order of magnitude, with the result from the easyFit method significantly overestimated and from the FlarEd method much overestimated compared to one from classical approach, with the result from the FlarEd method closer in absolute value. In all the cases, the FlareED method gave the results lower in absolute value compared to corresponding from the easyFit, for approximately 17.4%, 3.7% and 29.6% for these SFs, from lowest to highest in intensity, respectively. The results obtained based on the applied ML technique are in general very close to those obtained from the easyFit numerical method (Table 1), proving that this novel approach is as efficient as other two applied numerical



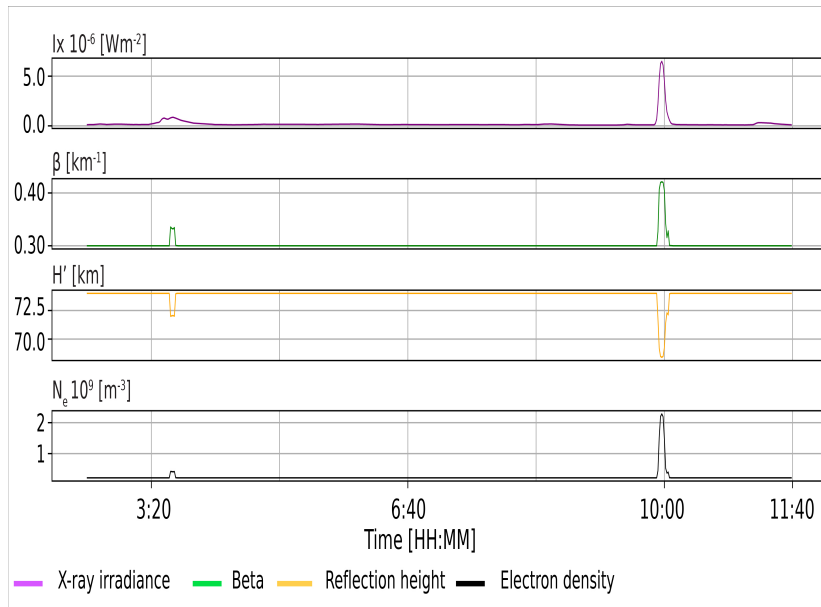


**Figure 7.** X-ray flux from GOES-15,  $\beta$  and  $H'$  parameters and  $N_e$  ( $h = 74$  km) as a function of UT during 23 December 2009 as results acquired by method relying on ML.

methods in the cases of low intensity SFs. The ML based approach gave the same electron density value in the case of B8.3 SF, slightly higher (for 0.99%) value in the case of C3.7 SF and somewhat lower value (for 2.15%) in the case of C6.4 SF. Figures 6-8 present output results from the applied ML workflow for these three SFs, with X-ray flux in violet, sharpness in green, reflection height in orange and estimated electron density in black.

#### 4. Summary

Overall, B - and C-class SFs occurring during solar minimum have a significant impact on the ionosphere. Impacts on the lower ionosphere of B - and C-class SFs during the 23/24 solar minimum has shed some light on the complex relationship between solar activity and Earth's upper atmosphere. Low class solar flares, although considered notably weaker in comparison to more powerful flares, still have the potential to significantly affect ionospheric dynamics especially during solar minimum periods. Understanding the ionospheric response to low intensity SFs during solar minimum is essential for understanding the potential adverse effects that such events can have on terrestrial communication systems and enhancing our overall space weather prediction capabilities.

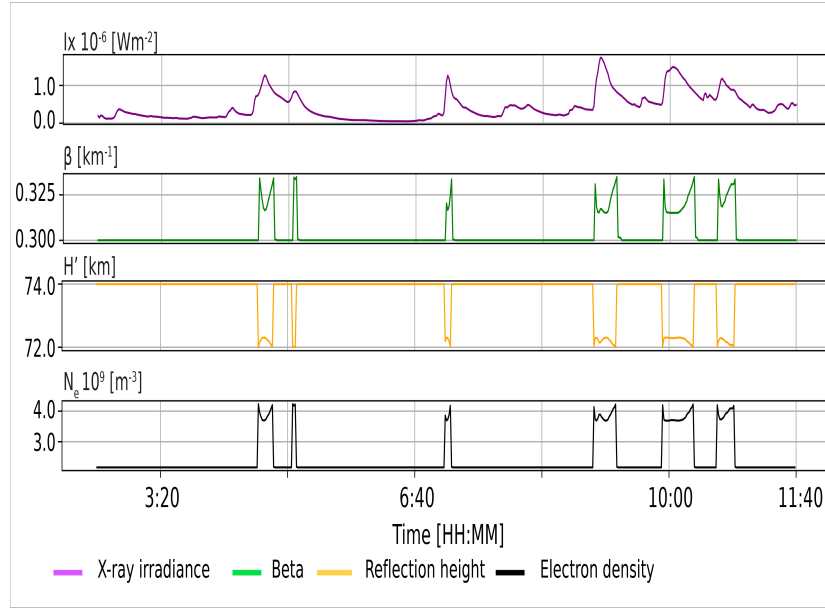


**Figure 8.** X-ray flux from GOES-15,  $\beta$  and  $H'$  parameters and  $N_e$  ( $h = 74$  km) as a function of UT during 27 October 2009 as results acquired by method relying on ML.

Numerical methods FlareED and easyFit were applied to SFs of low intensity ranging from B1 to C6.4 during seven selected days from period covering solar minimum between SCs 23 and 24, with the aim to test these two methods' efficiency and sensitivity when going through calculations related to SFs of low intensity, mainly from upper B-class and lower C-class solar X-ray flux. Both methods gave satisfactory results in terms of efficiency in cases of events stronger in intensity, with the easyFit method absolutely superior in cases of X-ray flux variations of very low intensity. A novel ML based approach gave results very similar to these obtained by easyFit method, giving great potential for applications in future studies.

When compared with results obtained from the classical approach using the LWPC methodology, in case of three SFs that cover the entire analyzed soft X-ray flux range (B8.3, C3.7 and C6.4) and can be taken as typical examples from their range, results obtained from FlareED method are lower in value compared to ones from easyFit. Compared to classical approach, in case of a) B8.3 SF  $N_e$ (easyFit) and  $N_e$ (FlareED) are for approximately 11% higher and 9% lower compared to  $N_e$ (LWPC), respectively. In case of b) C3.7  $N_e$ (easyFit) and  $N_e$ (FlareED) are for approximately 20% lower and 30% lower compared to  $N_e$ (LWPC), respectively. In case of c) C6.4 SF  $N_e$ (easyFit) and  $N_e$ (FlareED) are for approximately 99% higher (almost twice higher) and 40% higher compared to  $N_e$ (LWPC), respectively.

The findings from this research can potentially contribute to the development of improved forecasting models, enabling better prediction and preparedness for ionospheric disruptions caused by low class SFs. The study of low class SFs during solar minimum and their impact on the ionosphere highlights the need for continued research and monitoring of such events to enhance our understanding of space weather phenomena and protect technological infrastructure from potential disruptions.

**Acknowledgements.** This work was funded by the Institute of Physics Belgrade through a grant by the Ministry of Science, Technological Development and Innovations of the Republic of Serbia. Authors appreciate comments expressed by referees, which improved this paper.

## References

- Arnaut, F., Kolarski, A., & Srećković, V. A., Random Forest Classification and Ionospheric Response to Solar Flares: Analysis and Validation. 2023, *Universe*, **9**, DOI: 10.3390/universe9100436
- Barta, V., Natras, R., Srećković, V., et al. 2022, Multi-instrumental investigation of the solar flares impact on the ionosphere occurring in December 2006, Tech. rep., Copernicus Meetings
- Bothmer, V., Daglis, I. A., & Bogdan, T. J., Space Weather: Physics and Effects. 2007, *Physics Today*, **60**, 59, DOI: 10.1063/1.2825074
- Breiman, L., Random forests. 2001, *Machine learning*, **45**, 5
- Chen, T. & Guestrin, C., Xgboost: A scalable tree boosting system. 2016, in *Proceedings of the 22nd acm sigkdd international conference on knowledge discovery and data mining*, 785–794
- Curto, J. J., Geomagnetic solar flare effects: a review. 2020, *Journal of Space Weather and Space Climate*, **10**, 27, DOI: 10.1051/swsc/2020027
- Grodji, O. D. F., Doumbia, V., Amaechi, P. O., et al., A Study of Solar Flare Effects on the Geomagnetic Field Components during Solar Cycles 23 and 24. 2022, *Atmosphere*, **13**, 69, DOI: 10.3390/atmos13010069
- Grubor, D., Šulić, D., & Žigman, V., Classification of X-ray solar flares regarding their effects on the lower ionosphere electron density profile. 2008, *Annales Geophysicae*, **26**, 1731, DOI: 10.5194/angeo-26-1731-2008
- Hayes, L. A., O'Hara, O. S. D., Murray, S. A., & Gallagher, P. T., Solar Flare Effects on the Earth's Lower Ionosphere. 2021, *Solar Physics*, **296**, 157, DOI: 10.1007/s11207-021-01898-y
- Kelly, M. C. 2009, *The Earth's Ionosphere: Plasma Physics and Electrodynamics, Second Edition*
- Kolarski, A., Grubor, D., & Šulić, D., Diagnostics of the Solar X-Flare Impact on Lower Ionosphere through the VLF-NAA Signal Recordings. 2011, *Open Astronomy*, **20**, 591, DOI: 10.1515/astro-2017-0342

- Kolarski, A., Srećković, V. A., & Mijić, Z. R., Monitoring solar activity during 23/24 solar cycle minimum through VLF radio signals. 2022a, *Contributions of the Astronomical Observatory Skalnaté Pleso*, **52**, 105, DOI: 10.31577/caosp.2022.52.3.105
- Kolarski, A., Srećković, V. A., & Mijić, Z. R., Response of the Earth's Lower Ionosphere to Solar Flares and Lightning-Induced Electron Precipitation Events by Analysis of VLF Signals: Similarities and Differences. 2022b, *Applied Sciences*, **12**, 582, DOI: 10.3390/app12020582
- Ratcliffe, J. A. et al. 1972, *An introduction to ionosphere and magnetosphere* (CUP Archive, Cambridge, UK)
- Silber, I. & Price, C., On the use of VLF narrowband measurements to study the lower ionosphere and the mesosphere-lower thermosphere. 2017, *Surveys in Geophysics*, **38**, 407, DOI: 10.1007/s10712-016-9396-9
- Srećković, V. A., Šulić, D. M., Ignjatović, L., & Vujčić, V., Low Ionosphere under Influence of Strong Solar Radiation: Diagnostics and Modeling. 2021a, *Applied Sciences*, **11**, 7194, DOI: 10.3390/app11167194
- Srećković, V. A., Šulić, D. M., Vujčić, V., Jevremović, D., & Vykyuk, Y., The effects of solar activity: Electrons in the terrestrial lower ionosphere. 2017, *Journal of the Geographical Institute "Jovan Cvijic", SASA*, **67**, 221, DOI: 10.2298/IJGI1703221S
- Srećković, V. A., Šulić, D. M., Vujčić, V., Mijić, Z. R., & Ignjatović, L. M., Novel Modelling Approach for Obtaining the Parameters of Low Ionosphere under Extreme Radiation in X-Spectral Range. 2021b, *Applied Sciences*, **11**, 11574, DOI: 10.3390/app112311574
- Šulić, D. M. & Srećković, V. A., A Comparative Study of Measured Amplitude and Phase Perturbations of VLF and LF Radio Signals Induced by Solar Flares. 2014, *Serbian Astronomical Journal*, **188**, 45, DOI: 10.2298/SAJ1488045S
- Šulić, D. M., Srećković, V. A., & Mihajlov, A. A., A study of VLF signals variations associated with the changes of ionization level in the D-region in consequence of solar conditions. 2016, *Advances in Space Research*, **57**, 1029, DOI: 10.1016/j.asr.2015.12.025
- Wait, J. R. & Spies, K. P. 1964, *Characteristics of the Earth-ionosphere waveguide for VLF radio waves* (US Department of Commerce, National Bureau of Standards, Boulder, CO, USA)
- Žigman, V., Grubor, D., & Šulić, D., D-region electron density evaluated from VLF amplitude time delay during X-ray solar flares. 2007, *Journal of Atmospheric and Solar-Terrestrial Physics*, **69**, 775, DOI: <https://doi.org/10.1016/j.jastp.2007.01.012>